

Modeling of Lone Star Ticks with Deer Migration to Canada*

Jemisa Sadiku¹, Zilong Song^{1,†} and Jianhong Wu¹

Abstract Due to climate change and an increase of favourable habitat, ticks and tick-borne diseases are reported to expand to northern areas in north America. One main factor for lone star ticks to be established in Canada is due to the migration of white-tailed deers from US. In this work, we formulate a compartmental model to study the dynamics of lone star ticks and white-tailed deers, with a focus on migration effect of white-tailed deers. The tick-host interaction and the effect of deer migration are explored analytically and numerically. The positivity of the populations in the model is proved, and the unique positive equilibrium is proved to be asymptotically stable. We conduct sensitivity analysis on a set of parameters, revealing the correlation between the parameters and equilibrium populations. Numerical results show that migration rate of white-tailed deer is one crucial parameter that increases the populations of (infected) ticks and (infected) hosts.

Keywords Lone star tick, deer migration, disease modeling, asymptotic stability, sensitivity analysis.

MSC(2010) 37N25, 92D25, 92D30, 93D20.

1. Introduction

Lone star tick (*Amblyomma americanum*) is recognized for the first time by Linnaeus in 1758 [19]. It prefers damp forests and humid soil environment [30, 36]. Similar to other ticks, it has four life stages: egg, larvae, nymph and adult, and the transition from one stage to the next is done through questing, feeding and molting [3, 28, 33].

The associated tick-borne diseases and the allergic reaction have aroused increasing attention on lone star tick in recent years. Lone star tick is a vector that can carry pathogens and transmit tick-borne diseases such as STARI (Southern tick-associated rash illness) [10, 13] and Human Monocytic Ehrlichiosis (HME) [1, 19, 28] (CDC website). The preferred host (here white-tailed deer) also plays an important role in disease transmission, as they serve as reservoir for the pathogens. Unlike other species of ticks, lone star tick exhibits *aggressive* and indiscriminate questing behavior [13, 36], which makes bites to humans more likely. In addition, lone star tick causes red meat allergy (delayed-onset allergy) [22, 37], first discovered in

[†]the corresponding author.

Email address: jemisa.sadiku@gmail.com (J. Sadiku), buctsongzilong@163.com (Z. Song), wujhhida@gmail.com (J. Wu)

¹Department of Mathematics and Statistics, York University, Toronto, Ontario, Canada

*The authors were supported by Natural Science and Engineering Research Council Canada.

2009 [8]. The allergic reaction could be fatal [7, 21, 28], and is due to immunoglobulin E (IgE) antibody which is specific for galactose- α -1,3-galactose (alpha-gal). It is claimed that the cause of IgE antibodies is primary from bites of lone star tick [7].

The lone star tick is mostly found in the eastern, southeastern and south-central states of US [32]. However, its distribution and abundance have increased over the past decades, and according to CDC map it expands to more northern and western areas in North America where it was absent in previous years [32]. In particular, it has migrated from endemic areas in the US to new regions in Southern Canada, such as British Columbia, Ontario, south-eastern Manitoba [6, 28, 29].

Two main factors responsible for the range expansion of lone star ticks are the climate change and the migration of white-tailed deer [32]. Due to climate change, more regions become inhabitable for lone star ticks. Since ticks are small species, they will spread to new regions mainly by migration of their host mammals. White-tailed deer is the main host for lone star tick of all life stages to get the majority of their blood meals, and their populations are positively correlated [3, 6, 18, 28]. The deer migration depends on the deer habitat suitability of the region, which is influenced by two factors: the need for food, shelter and water, and the disturbances from human activities (such as hunting) [6]. In order to better understand or predict the outbreaks of tick-borne diseases, there is need to include the migration effect into the tick-host dynamics.

Various models have been proposed to investigate tick-host dynamics and to address a variety of issues on the tick-borne diseases [25, 38]. Specifically for Lone star ticks, there have been computer simulations based on age-structured difference equations [15, 27], agent-based models [34], predicative statistical models [20]. Recently, a metapopulation model with migration effect among patches and logistic-type birth term is adopted in [11, 12] to study the HME transmission and investigate various tick-control strategies. For another tick-borne disease (Lyme disease) [25], the range expansion of ticks and pathogens has been widely studied by various migration effects including movements of rodents and deer [5] as well as bird migration [16]. The migration of white-tailed deer has also been included in a single patch model with distributed delay (integral) term [2], which models that the deer travels out and then back in the patch. Since the logistic-type birth term may cause negative birth rate at high population density (which could occur with migration effect), other positive density-dependent birth rates have been adopted in modeling of ticks [33, 39].

In this paper, we formulate a compartment model, where the hosts and ticks have been divided into susceptible and infected compartments. Our model adopts the Ricker function as the birth term to ensure positivity, which was used in a stage-structured model [39]. It also includes a simple migration term in the dynamics of hosts, with a focus to study the migration effects of white-tailed deer from US to Canada. The positivity of the populations in the model is proved with natural biologically meaningful parameters. With migration effect as a source term, there exists a unique positive equilibrium, which is asymptotically stable. Our numerical results confirms these features and sensitivity analysis is carried out to reveal the effects of parameters. Migration rate is found to be a crucial parameter that increases the populations of (infected) ticks and (infected) hosts.

The rest of the manuscript is arranged as follows. The mathematical model is proposed in Section 2. After non-dimensionalization, Section 3 proves the positivity of the solutions and the stability of the unique positive equilibrium. In Section 4,

numerical results and sensitivity analysis are carried out, and the effects of parameters including migration rate are studied. Finally, conclusions and future extensions are provided in Section 5.

2. The mathematical model

Given that lone star tick prefers white-tailed deer as the main host for all life stages [12], we formulate a mathematical model with a single host. We neglect the life stages of tick, and restrict ourselves to a single life stage, although the stage structure will be included in a later study. For simplicity, seasonality [23] has been ignored in the model, but it can be reflected by varying the parameters in the model. We concentrate on a single patch (region in Canada), and there is migration of host from the outside environment (US) where the host population is assumed as a constant.

Table 1. Definition and values of parameters

Symbol	Meaning	Value and Reference
b	Birth rate of host	0.2/month [12, 35]
q	Strength of density dependence for host birth	1/100 [est]
β	Transmission rate from infected tick to susceptible host	0.02/month [11, 12]
μ	Death rate of host	0.01/month [12, 35]
m	Migration rate from outside region to current region	0.01/month [11]
\hat{b}	Birth rate of ticks	0.75/month [12]
\hat{q}	Strength of density dependence for tick birth	1/20000 [11]
$\hat{\mu}$	Death rate of ticks	0.1/month [12]
$\hat{\beta}$	Transmission rate from infected host to susceptible tick	0.07/month [11, 12]
N_a	Average number of ticks per host	100 [11, 12]
r_s	Ratio of infected ticks over all ticks on susceptible host	0.05 [est]
r_I	Ratio of infected ticks over all ticks on infected host	0.1 [est]
H_s^o	Population of susceptible host in the outside region	800 [est]
H_I^o	Population of infected host in the outside region	200 [est]

The susceptible host and susceptible tick are denoted by H_s and T_s , and the infected host and infected tick are denoted by H_I and T_I . A flow chart is depicted in Figure 1. Correspondingly, the model is given by

$$\frac{dH_s}{dt} = b(H_s + H_I)e^{-q(H_s+H_I)} - \mu H_s - \beta \frac{H_s}{H_s + H_I} T_I + m H_s^o, \quad (2.1a)$$

$$\frac{dH_I}{dt} = \beta \frac{H_s}{H_s + H_I} T_I - \mu H_I + m H_I^o, \quad (2.1b)$$

$$\begin{aligned} \frac{dT_s}{dt} = & \hat{b}(T_s + T_I)e^{-\hat{q}(T_s+T_I)} - \hat{\mu} T_s - \hat{\beta} N_a \frac{T_s}{T_s + T_I} H_I \\ & + (1 - r_s) N_a m H_s^o + (1 - r_I) N_a m H_I^o \end{aligned} \quad (2.1c)$$

$$\frac{dT_I}{dt} = \hat{\beta} N_a \frac{T_s}{T_s + T_I} H_I - \hat{\mu} T_I + r_s N_a m H_s^o + r_I N_a m H_I^o, \quad (2.1d)$$

where the physical meanings of the parameters are given in Table 2, with typical values based on other works in the literature. The Ricker function [39] is used for

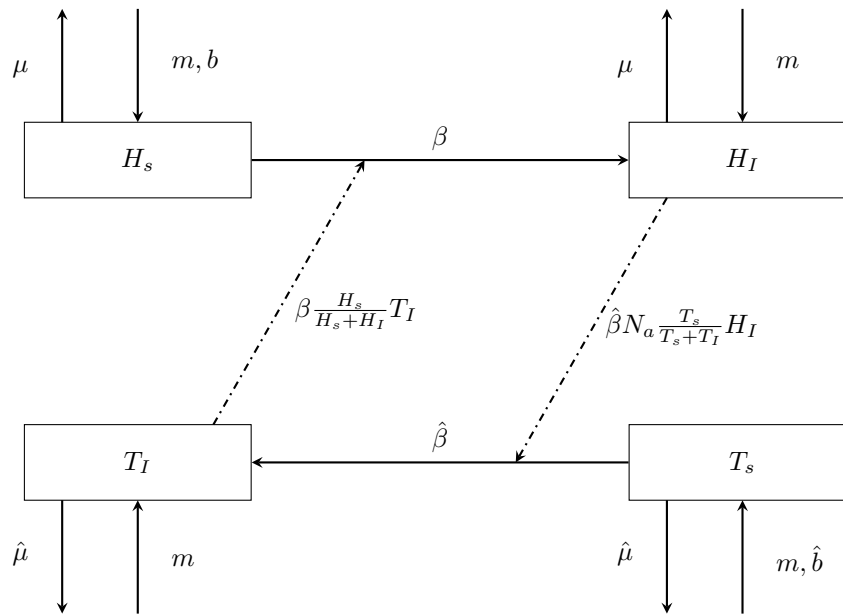


Figure 1. Flow chart for the compartmental model.

the birth term of both tick and host. The death rate for infected and susceptible hosts are assumed to be a common constant μ , and that for all ticks are assumed to be $\hat{\mu}$. Hereafter, a parameter with a hat symbol is associated with ticks. We assume that the transmission of disease occurs only from ticks to host or from host to tick, but not from tick to tick (such as cofeeding [24, 40]) or from host to host. The migration of host to the concerned region (Canada) is proportional to the host population in the outside region (US) with a migration rate m , since the outside region is assumed to have a much larger population size for host. The ratio of infected ticks over all ticks on susceptible host is r_s and that on infected hosts is r_I . The value of r_I could be greater than r_s since the host is more likely to be in the infected state if there are more infected ticks feeding on it.

For convenience, we denote total populations of ticks and hosts as

$$T = T_s + T_I, \quad H = H_s + H_I, \quad H^o = H_s^o + H_I^o, \quad (2.2)$$

where superscript o means the outside region. By (2.1), the equivalent system for (H, T, H_I, T_I) is given by

$$\frac{dH}{dt} = bHe^{-qH} - \mu H + mH^o, \quad (2.3a)$$

$$\frac{dT}{dt} = \hat{b}Te^{-\hat{q}T} - \hat{\mu}T + N_a m H^o, \quad (2.3b)$$

$$\frac{dH_I}{dt} = \beta \frac{H - H_I}{H} T_I - \mu H_I + m H_I^o, \quad (2.3c)$$

$$\frac{dT_I}{dt} = \hat{\beta} N_a \frac{T - T_I}{T} H_I - \hat{\mu} T_I + (r_s H_s^o + r_I H_I^o) N_a m. \quad (2.3d)$$

Based on the physical meaning of the parameters (see Table 2), we naturally

have the following restrictions

$$\begin{aligned} b > 0, \quad \mu > 0, \quad \hat{b} > 0, \quad \hat{\mu} > 0, \quad \beta > 0, \quad \hat{\beta} > 0, \\ q > 0, \quad \hat{q} > 0, \quad N_a > 0, \quad 0 < r_s < 1, \quad 0 < r_I < 1, \\ m > 0, \quad H^o > H_I^o > 0, \quad H^o > H_s^o > 0. \end{aligned} \quad (2.4)$$

3. Positivity and equilibrium analysis

In this section, we first do the non-dimensionalization to identify the effective combination of parameters. Then, we show the positivity of solutions, which is a crucial property of a biological system. Finally, we analyze the equilibrium of the system and its stability.

3.1. Non-dimensionalization

Now we simplify the system in (2.3) by using the scales

$$\tilde{H} = qH, \quad \tilde{H}_I = qH_I, \quad \tilde{T} = \hat{q}T, \quad \tilde{T}_I = \hat{q}T_I, \quad \tilde{t} = bt. \quad (3.1)$$

Then we can get the dimensionless system for $\tilde{H}, \tilde{T}, \tilde{H}_I, \tilde{T}_I$. To make the system easier to read we drop the tilde, and the dimensionless system is

$$\frac{dH}{dt} = He^{-H} - s_1H + s_2, \quad (3.2a)$$

$$\frac{dT}{dt} = s_3Te^{-T} - s_4T + s_5, \quad (3.2b)$$

$$\frac{dH_I}{dt} = s_6\left(1 - \frac{H_I}{H}\right)T_I - s_1H_I + s_7, \quad (3.2c)$$

$$\frac{dT_I}{dt} = s_8\left(1 - \frac{T_I}{T}\right)H_I - s_4T_I + s_9, \quad (3.2d)$$

where the dimensionless parameters are given by

$$\begin{aligned} s_1 &= \frac{\mu}{b}, \quad s_2 = \frac{qmH^o}{b}, \quad s_3 = \frac{\hat{b}}{b}, \quad s_4 = \frac{\hat{\mu}}{b}, \quad s_5 = \frac{\hat{q}N_a m H^o}{b}, \\ s_6 &= \frac{\beta q}{b\hat{q}}, \quad s_7 = \frac{qmH_I^o}{b}, \quad s_8 = \frac{N_a\hat{\beta}\hat{q}}{bq}, \quad s_9 = \frac{\hat{q}N_a m (r_s H_s^o + r_I H_I^o)}{b}. \end{aligned} \quad (3.3)$$

Then by (3.2) and definition of H_s and T_s , the corresponding equation for H_s and T_s will be

$$\begin{aligned} \frac{dH_s}{dt} &= He^{-H} - s_6 \frac{H_s}{H} (T - T_s) - s_1H_s + s_2 - s_7, \\ \frac{dT_s}{dt} &= s_3Te^{-T} - s_8 \frac{T_s}{T} (H - H_s) - s_4T_s + s_5 - s_9. \end{aligned} \quad (3.4)$$

From the conditions of parameters in (2.4), we have the natural restrictions for the dimensionless parameters

$$s_i > 0, \quad (i = 1, \dots, 9), \quad s_2 > s_7, \quad s_5 > s_9. \quad (3.5)$$

3.2. Positivity of Solutions

In this subsection, we show the positivity of the solutions with initial positive data. To this end, we define the two sets:

$$\begin{aligned} S &= \{(T, H, T_I, H_I) | T > 0, H > 0, T_I > 0, H_I > 0\}, \\ \hat{S} &= \{(T_s, H_s, T_I, H_I) | T_s > 0, H_s > 0, T_I > 0, H_I > 0\}. \end{aligned} \quad (3.6)$$

The aim is to show the two sets are invariant. The invariance of \hat{S} implies the invariance of S , but the reverse is not true, e.g., positive H and H_I can not imply positive $H_s = H - H_I$.

Theorem 3.1. *With the natural restrictions of parameters in (3.5) for the systems in (3.2) and (3.4), or equivalently with conditions (2.4) for the original systems in (2.3) and (2.1), the two sets S and \hat{S} are invariant.*

Proof. First, we show that the set S is invariant. As Eq. (3.2a) is decoupled from the system, the positivity of H can be analyzed separately. We denote the right-hand side as

$$f(H) := He^{-H} - s_1H + s_2, \quad (3.7)$$

and get

$$\frac{dH}{dt} = f(H) \rightarrow s_2 > 0, \quad \text{as } H \rightarrow 0. \quad (3.8)$$

Thus, the quantity H remains positive. In fact, even for the case $s_2 = 0$ (or $m = 0$), one can show the positivity of H , by using the equivalent equation

$$\frac{d(He^{s_1t})}{dt} = He^{-H+s_1t} > 0, \quad \text{for } H > 0. \quad (3.9)$$

Similarly, T remains positive by Eq. (3.2b). We further show that the H and T are bounded, before proving the positivity of H_I and T_I . Clearly by (3.8), H is bounded from below, say $H \geq H_{min} > 0$. Note that

$$f(H) \rightarrow -\infty, \quad \text{as } H \rightarrow \infty, \quad (3.10)$$

then there exists a $H_{max} \geq H(0) > 0$ such that

$$\frac{dH}{dt} = f(H) < 0, \quad \text{for } H \geq H_{max}. \quad (3.11)$$

Therefore, we obtain $H \in [H_{min}, H_{max}]$, where in some cases H_{min} or H_{max} could be $H(0)$. Similarly T is bounded. With the boundedness, we get

$$\begin{aligned} H_I/H &\rightarrow 0, \quad \text{as } H_I \rightarrow 0, \\ T_I/T &\rightarrow 0, \quad \text{as } T_I \rightarrow 0. \end{aligned} \quad (3.12)$$

Subsequently in the first quadrant of the plane of (H_I, T_I) , we obtain

$$\begin{aligned} \frac{dH_I}{dt} &\rightarrow s_6T_I + s_7 > 0, \quad \text{as } H_I \rightarrow 0, \\ \frac{dT_I}{dt} &\rightarrow s_8H_I + s_9 > 0, \quad \text{as } T_I \rightarrow 0. \end{aligned} \quad (3.13)$$

So, the two quantities H_I and T_I will remain positive.

Next, we prove the positivity of H_s and T_s , or equivalently the invariance of \hat{S} . We note that H and T are positive and bounded, independent of dynamics of H_s and T_s in (3.4). Each of the terms He^{-H} and Te^{-T} has a minimum positive value. Then, we have

$$\begin{aligned}\frac{dH_s}{dt} &\geq He^{-H} + s_2 - s_7 > 0, \quad \text{as } H_s \rightarrow 0, \\ \frac{dT_s}{dt} &\geq s_3Te^{-T} + s_5 - s_9 > 0, \quad \text{as } T_s \rightarrow 0,\end{aligned}\tag{3.14}$$

which implies positivity of H_s and T_s and hence the invariance of \hat{S} . \square

Remark 3.1. In the current model, we have used the Ricker's function He^{-H} for the birth term to ensure its positivity, which is essential for the positivity of H_s . A logistic-type birth term $H(1-H)$ (after non-dimensionlization) often appears in other tick models [11, 12], but with current migration effect such a term may give a negative birth rate, since $H > 1$ is possible with certain parameters.

3.3. Equilibrium analysis

Theorem 3.2. *With the natural conditions (3.5) for the system in (3.2), there exists a unique positive equilibrium (H^*, T^*, H_I^*, T_I^*) , which is asymptotically stable.*

Proof. (1) As the equations for H and T are decoupled from the system, we first show the equilibrium of H and T . We take Eq. (3.5a) for example. With the definition (3.7), we see that

$$f(0) = s_2 > 0, \quad f(\infty) = -\infty,\tag{3.15}$$

thus there exists at least one positive root (equilibrium). Taking the derivative gives

$$f'(H) = (1-H)e^{-H} - s_1, \quad f'(0) = 1 - s_1.\tag{3.16}$$

There are two cases: $s_1 \geq 1$ and $0 < s_1 < 1$. When $s_1 \geq 1$, we always have

$$f'(H) < e^{-H} - s_1 < 0, \quad \text{for } H > 0.\tag{3.17}$$

This implies $f(H)$ is monotone decreasing, and by (3.15) there exists a unique positive root. For the case $0 < s_1 < 1$, the $f'(H)$ is positive for small H by (3.16). Note that

$$f'(1) = -s_1 < 0,\tag{3.18}$$

so there exists a critical value $0 < H_c < 1$ such that

$$\begin{aligned}f'(H_c) &= (1-H_c)e^{-H_c} - s_1 = 0, \\ f'(H) &> 0, \quad \text{for } 0 < H < H_c.\end{aligned}\tag{3.19}$$

Taking the second derivative gives

$$f''(H) = (H-2)e^{-H} < 0, \quad \text{for } H_c < H < 1,\tag{3.20}$$

which implies $f'(H)$ is decreasing in the above interval and

$$f'(H) < 0, \quad \text{for } H_c < H < 1.\tag{3.21}$$

It is clear from (3.16) that

$$f'(H) = (1 - H)e^{-H} - s_1 < 0, \quad \text{for } H \geq 1. \quad (3.22)$$

Combining (3.19,3.21,3.24), we conclude that $f(H)$ is increasing in $[0, H_c)$ and is decreasing in (H_c, ∞) . Therefore, $f(H)$ has a unique positive root in (H_c, ∞) . We denote the root (equilibrium) by H^* , then based on the above analysis, in either case we always have

$$\begin{aligned} f(H) &> 0 \quad \text{for } 0 < H < H^*, \\ f(H) &< 0 \quad \text{for } H > H^*. \end{aligned} \quad (3.23)$$

Therefore, the equilibrium H^* is (globally) asymptotically stable.

Similar arguments apply to the function for T , by defining

$$g(T) = Te^{-T} - \frac{s_4}{s_3}T + \frac{s_5}{s_3}, \quad (3.24)$$

where s_1 and s_2 are replaced by the two fractions s_4/s_3 and s_5/s_3 . Therefore the unique equilibrium, denoted by T^* , is (globally) asymptotically stable.

(2) Next we show the equilibrium of (H_I, T_I) and its local stability. The theory of asymptotically autonomous systems [9] implies that one can substitute the equilibria H^*, T^* into the system for T_I, H_I for the equilibrium analysis. By coupling the two equations (3.2c) and (3.2d), the equilibrium of H_I is determined by

$$\begin{aligned} AH_I^2 + BH_I + C &= 0, \\ A &= -\frac{s_6s_8}{H^*} - \frac{s_1s_8}{T^*} < 0, \\ B &= B_1 + B_2 = \left(\frac{s_7s_8}{T^*} - \frac{s_6s_9}{H^*}\right) + (s_6s_8 - s_1s_4), \\ C &= s_4s_7 + s_6s_9 > 0, \end{aligned} \quad (3.25)$$

where B_1 and B_2 are defined in the two brackets. Then, there exist two roots, one positive and one negative, denoted by $H_I^{(1)} > 0$ and $H_I^{(2)} < 0$. Similarly, the equilibrium of T_I is given by

$$\begin{aligned} \hat{A}T_I^2 + \hat{B}T_I + \hat{C} &= 0, \\ \hat{A} &= -\frac{s_6s_8}{T^*} - \frac{s_4s_6}{H^*} < 0, \\ \hat{B} &= -B_1 + B_2, \\ \hat{C} &= s_7s_8 + s_1s_9 > 0. \end{aligned} \quad (3.26)$$

The two roots (equilibria) are denoted by $T_I^{(1)} > 0$ and $T_I^{(2)} < 0$. Furthermore, by equations (3.2c) and (3.2d), the two variables H_I and T_I at equilibrium are connected by a linear equation

$$B_1 + AH_I - \hat{A}T_I = 0, \quad (3.27)$$

with the same parameters B_1, A, \hat{A} as above. Then, the two roots $T_I^{(1)}, T_I^{(2)}$ and those $H_I^{(1)}, H_I^{(2)}$ are related by this linear relation, so they form two pairs. Since $A < 0$ and $\hat{A} < 0$, the larger solution of H_I corresponds to the larger solution of

T_I and hence the positive $T_I^{(1)}$ (or negative $T_I^{(2)}$) corresponds to the positive $H_I^{(1)}$ (or negative $H_I^{(2)}$). Therefore, we conclude that there is a unique pair of positive equilibria, denoted by $T_I^* = T_I^{(1)}$ and $H_I^* = H_I^{(1)}$.

For the system of (3.2c) and (3.2d), the local stability of the equilibrium (H_I^*, T_I^*) is determined by the eigenvalues of the matrix

$$D_I = \begin{pmatrix} -s_1 - s_6 \frac{T_I^*}{H_I^*}, & s_6(1 - \frac{H_I^*}{H_I^*}) \\ s_8(1 - \frac{T_I^*}{T_I^*}), & -s_4 - s_8 \frac{H_I^*}{T_I^*} \end{pmatrix}. \tag{3.28}$$

By the conditions (3.5) and positivity of equilibrium, we easily get

$$\text{Tr}(D_I) = -s_1 - s_6 \frac{T_I^*}{H_I^*} - s_4 - s_8 \frac{H_I^*}{T_I^*} < 0. \tag{3.29}$$

Then, the equilibrium is asymptotically stable if $\text{Det}(D_I) > 0$, which can be expressed by

$$-B_2 - AH_I^* - \hat{A}T_I^* > 0. \tag{3.30}$$

By (3.27), it is equivalent to

$$B + 2AH_I^* < 0, \quad (\text{or } \hat{B} + 2\hat{A}T_I^* < 0). \tag{3.31}$$

Since H_I^* is the positive root (the larger one) of quadratic equation in (3.25), we get

$$B + 2AH_I^* = -\sqrt{B^2 - 4AC} < 0. \tag{3.32}$$

This means the condition (3.30) automatically holds, and hence the equilibrium (H^*, T^*) is asymptotically stable. \square

Remark 3.2. Theorems 3.1 and 3.2 imply that there exists a unique positive equilibrium $(H_s^*, H_I^*, T_s^*, T_I^*)$ for the original system (2.1), where $H_s^* = H^* - H_I^*$, $T_s^* = T^* - T_I^*$.

Remark 3.3. The above theorem deals with the case $m > 0$, now we compare it with the critical case $m = 0$. With $m = 0$, from the definitions (3.3, 3.25, 3.26) we have

$$s_2 = s_5 = s_7 = s_9 = 0, \quad C = \hat{C} = 0. \tag{3.33}$$

With $s_1 < 1$ (i.e., $\mu < b$) and $s_3 < s_4$ (i.e., $\hat{\mu} < \hat{b}$), there still exists a unique positive equilibrium (H^*, T^*) for the system of (H, T) , which is asymptotically stable. For the system of (T_I, H_I) , clearly there is a disease free equilibrium, $T_I = 0, H_I = 0$. The stability of this equilibrium (0,0) is determined by (see (3.30))

$$-B_2 > 0, \quad \Leftrightarrow \quad s_1 s_4 - s_6 s_8 > 0, \quad \Leftrightarrow \quad R_0 \equiv \frac{\beta \hat{\beta} N_a}{\mu \hat{\mu}} < 1. \tag{3.34}$$

If $R_0 < 1$, the equilibrium (0,0) is stable, and there is no positive equilibrium with $m = 0$ (the other equilibrium is negative). As m increases from 0, the positive equilibrium in the theorem is a perturbation of the disease free equilibrium. If $R_0 > 1$, the equilibrium (0,0) is unstable, but there is the other positive equilibrium with $m = 0$, denoted by (T_{I0}^*, H_{I0}^*) , which is asymptotically stable. As m increases from 0, the positive equilibrium in the theorem is a perturbation of (T_{I0}^*, H_{I0}^*) . If $R_0 = 1$, this (T_{I0}^*, H_{I0}^*) coincides with (0,0). In brief, the positive equilibrium with $m > 0$ is always a perturbation of the stable equilibrium with $m = 0$.

4. Numerical results and sensitivity analysis

In this section, we present the solutions with typical parameters. Then, we conduct the sensitivity analysis for some parameters. Finally, the effects of migration rate and death rates are further analyzed.

4.1. Solution curves

To simulate the dynamics of the system (2.3), we adopt the initial values as in [11]

$$H(0) = 10, \quad T(0) = 3000, \quad H_I(0) = 8, \quad T_I(0) = 80. \quad (4.1)$$

The initial values are based on one patch of $10,000 \text{ m}^2$ in [11], and other parameters used in simulation are shown in table 1. In Table 1, q is estimated from the carrying capacity of host, and we set $\hat{q} = q/M, N_a = M/2$, where $M = 200$ is maximum number of ticks per host in [11, 12]. Other estimated parameter are also consistent with this setting. If we were to consider a larger region, we could multiply a factor on these initial values and modify the estimated parameters q, \hat{q} and H_I^o, H_s^o .

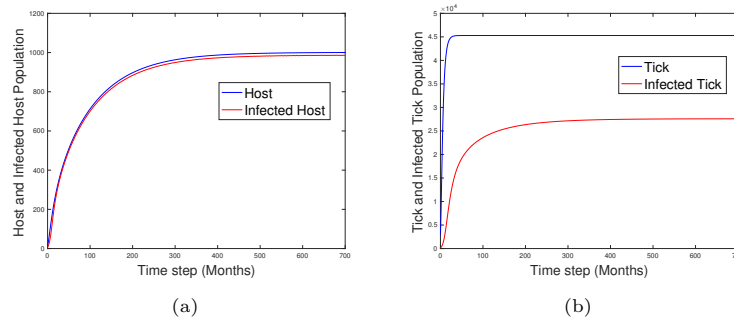


Figure 2. The dynamic curves for (a) host H and infected host H_I , (b) tick T and infected tick T_I .

Figure 2 shows the dynamics for the populations of host, tick, infected host and infected tick, with parameters in Table 1. All the four populations quickly reach the positive equilibrium. To see more clearly the effect of migration rate m in the two different cases in Remark 3.3, the dynamics of the infected host and infected ticks are shown in Figures 3 and 4 with varying parameters. With parameters in table 1, we have $R_0 = \frac{\beta\hat{\beta}N_a}{\mu\hat{\mu}} = 140 > 1$, and Figure 3 shows the dynamics of H_I, T_I by varying m . Initially with $m = 0$, there is stable positive equilibrium, and as m increases the positive equilibrium increases. By changing μ from 0.01 to 0.1 (due to hunting or predators) and $\hat{\mu}$ from 0.1 to 0.5 (due to tick control measures) and setting $N_a = 25$, we get $R_0 = 0.7 < 1$, and Figure 4 shows the dynamics of H_I, T_I by varying m . Initially with $m = 0$, there is a stable disease free equilibrium $(0,0)$, but as m increases this equilibrium increases as the positive equilibrium for the case $m > 0$. This verifies the analysis in Remark 3.3.

4.2. Sensitivity Analysis

The mathematical analysis about the equilibrium and its stability can answer the questions about the long time behaviour, with fixed parameters. However, we have

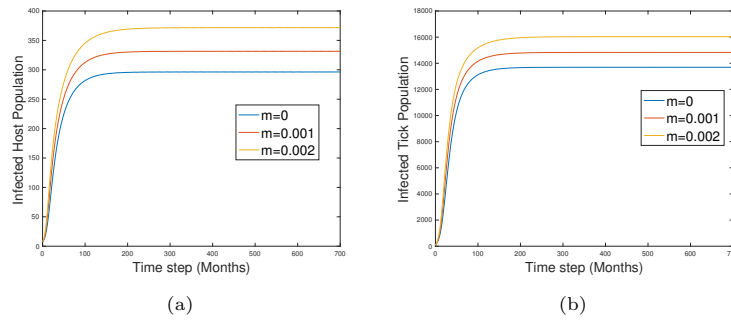


Figure 3. The dynamic curves for infected host H_I and infected tick T_I with varying $m = 0, 0.001, 0.002$ ($R_0 = 140$ for the case $m = 0$).

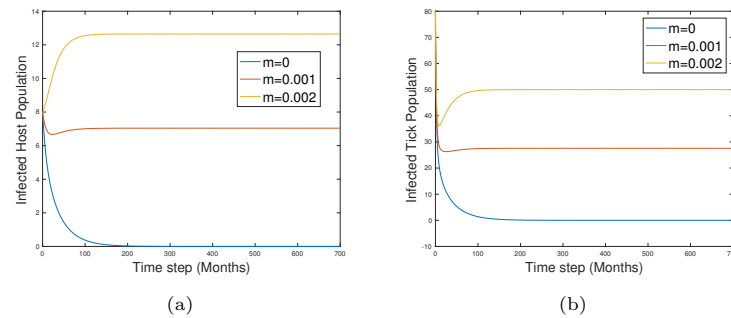


Figure 4. The dynamic curves for infected host H_I and infected tick T_I with varying $m = 0, 0.001, 0.002$ ($R_0 = 0.7$ for the case $m = 0$).

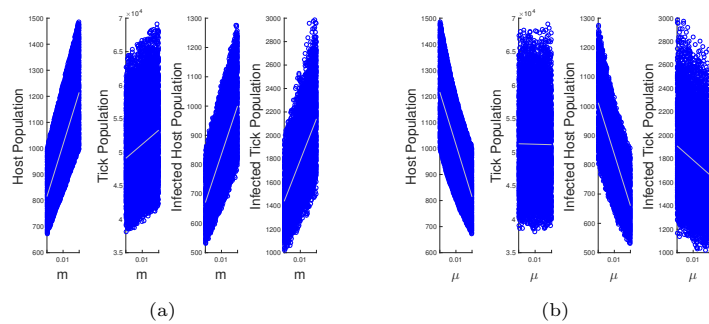


Figure 5. The scatter plot between the four equilibrium populations (H^*, T^*, H_I^*, T_I^*) and two parameters m and μ by LHS.

made assumptions about the parameters and there is always uncertainty in the estimation of parameters, which will result in uncertainty of the results. The Latin Hypercube Sampling (LHS) and Partial Rank Correlation Coefficient (PRCC) provides a useful tool to analyze a range of parameters and its effects on the dynamics/equilibrium of populations [4, 14, 26].

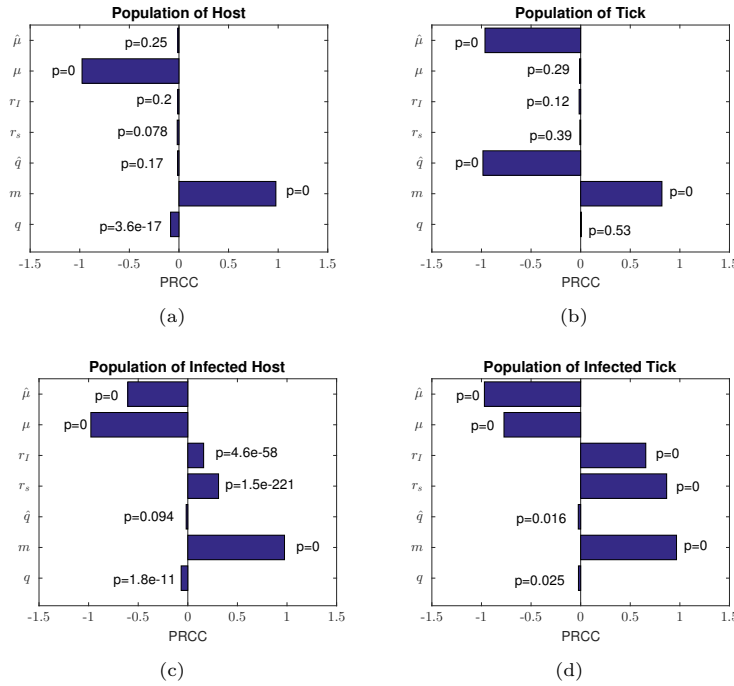


Figure 6. The PRCC results for four equilibrium populations (H^* , T^* , H_I^* , T_I^*) against parameters m , μ , $\hat{\mu}$, q , \hat{q} , r_s and r_I .

In the first step, we carry out the LHS, and verify the monotone relationship to ensure that the selected range of parameters are suitable for the PRCC analysis. We take m and μ for illustration, and other parameters such as r_s , r_I , $\hat{\mu}$ etc. are similarly verified but omitted here for brevity. We set the range of the parameters to be a 20% change of the value in Table 1, i.e., $m \in [0.008, 0.012]$ and $\mu \in [0.008, 0.012]$. Uniform distribution is used in the LHS and 10,000 parameter sets are generated. Figure 5 shows the scatter plots for the equilibrium of four populations with respect to the two parameters m and μ in the parameter sets. Each point in the figure is from a simulation with one parameter set. One can see that all the subfigures show an increasing or decreasing pattern, except the tick population in Figure 5(b), since tick population T does not depend on μ by Eq. (2.3b). This suggests that the selected range of parameters can be used to perform the PRCC analysis.

Next we calculate the PRCC, which determines how much each input parameter contributes to the output variable or measure. Figure 6 shows the PRCC results between the equilibrium of four populations and seven parameters m , μ , $\hat{\mu}$, q , \hat{q} , r_s , r_I . The approximate p -values are shown inside the figure, and $p < 0.01$ means significant result. For significant result, the positive or negative PRCC value indicates

a positive or negative correlation between the parameter and the output [26]. In Figure 6, the migration rate m is significant for all four equilibrium populations, and is positively correlated with them. The parameters μ (major effect) and q (minor effect) are negatively correlated with the equilibrium host population H^* , while $\hat{\mu}$ and \hat{q} negatively affect the equilibrium tick population T^* . Both death rates μ and $\hat{\mu}$ are negatively correlated with the equilibrium infected host and infected tick populations, as there is strong coupling in the two equations of H_I and T_I . The parameters r_I, r_s have a major positive correlation with equilibrium infected tick population T_I^* , as they directly appear in (2.3d), and they have a minor positive effect on equilibrium infected host population H_I^* due to the interactions of T_I and H_I .

4.3. The effects of migration rate and death rates

We further analyze effects of migration rate m and death rates $\mu, \hat{\mu}$ on the equilibrium populations for two reasons. First, the sensitivity analysis shows that these parameters are significant for the equilibrium populations. Second, these are related to practical control measures [17], and can provide insights on the future policy making. The migration rate m is affected by border control and deer habitat suitability [6]. The death rate of host is influenced by its predators and the hunting activities [36]. The death rate of ticks is affected by seasonality and temperature and can also be controlled by use of acaricide [12, 31].

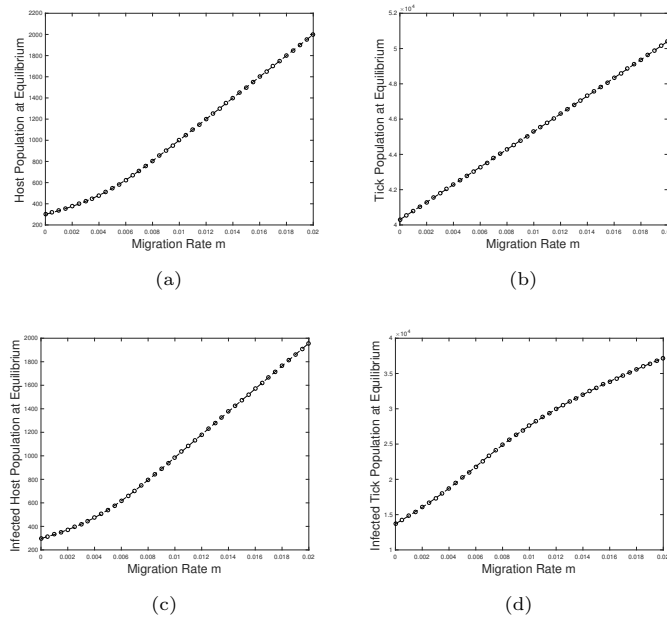


Figure 7. The dependence of equilibrium populations on migration rate m : (a) host H^* , (b) tick T^* , (c) infected host H_I^* , (d) infected tick T_I^* .

Figure 7 shows the dependence of the four equilibrium populations on migration rate m , indicating a positive correlation. This is consistent with the previous anal-

Table 2. Effect of migration rate.

Population	slope at $m = 0.01$	change by increasing m by 10%
Host	9.92×10^4	9.94%
Tick	5.04×10^5	1.11%
Infected host	9.70×10^4	9.86%
Infected tick	1.26×10^6	4.41%

ysis and PRCC results. Table 2 presents the slope of the curve at $m = 0.01$ and the relative change of population with increase of m by 10%. It shows about 10% increase for the host populations H^* and H_I^* , which is significant. It also positively affects tick populations T^* and T_I^* . The dependence on m can also be directly obtained based on previous analysis, for example, we get

$$\frac{dH^*}{dm} = \frac{H^o}{\mu + be^{-qH^*}(qH^* - 1)}, \quad \frac{dT^*}{dm} = \frac{H^o N_a}{\hat{\mu} + \hat{b}e^{-\hat{q}T^*}(\hat{q}T^* - 1)}. \quad (4.2)$$

With the chosen parameters and equilibrium values in Figure 2, we obtain exactly the results in Table 2. This verifies the results in this section. The formulas for the slopes dH_I^*/dm and dT_I^*/dm are complicated and hence omitted here.

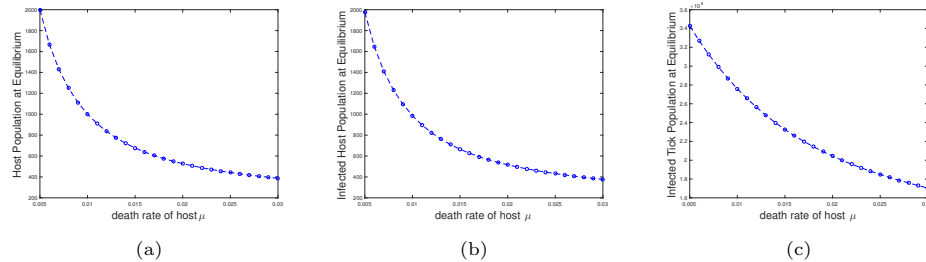


Figure 8. The dependence of equilibrium populations on death rate of host μ : (a) host H^* , (b) infected host H_I^* , (c) infected tick T_I^* .

Table 3. Effect of death rate of host.

Population	slope at $\mu = 0.01$	change by increasing μ by 10%
Host	-9.91×10^4	-8.99%
Tick	0	0%
Infected host	-9.83×10^4	-9.04%
Infected tick	-1.07×10^6	-3.71%

The dependence of the equilibrium populations on death rate of host μ is presented in Figure 8 and Table 3. The death rate μ has a negative correlation with the three populations H^* , H_I^* and T_I^* . It significantly affects H^* and H_I^* , which decrease by 8.99% and 9.04% with an increase of μ by 10%. The T^* - μ subfigure (a

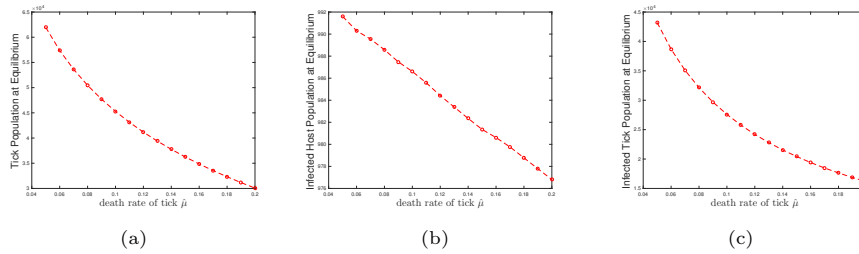


Figure 9. The dependence of equilibrium populations on death rate of tick $\hat{\mu}$: (a) tick T^* , (b) infected host H_I^* , (c) infected tick T_I^* .

constant) is omitted in Figure 8, since there is no correlation between T^* and μ , indicated by 0% in Table 3. This is because in the present model the birth term of ticks in (2.3b) does not depend on the host population H , although H could be included in the parameter \hat{q} in future work.

Table 4. Effect of death rate of tick.

Population	slope at $\hat{\mu} = 0.1$	change by increasing $\hat{\mu}$ by 10%
Host	0	0%
Tick	-2.28×10^5	-4.77%
Infected host	-96.8	-0.1%
Infected tick	-1.94×10^5	-6.57%

Figure 9 and Table 4 show the effects of death rate of tick $\hat{\mu}$. The parameter $\hat{\mu}$ has a negative correlation with the three populations T^*, H_I^*, T_I^* , and has no relation with H^* . It has most significant impact on T_I^* , with a 6.57% decrease with increase of $\hat{\mu}$ by 10 %.

5. Conclusions

In this work, we have formulated a compartmental model for lone star ticks and white-tailed deers, where a Ricker function is adopted for birth term and the migration effect is emphasized. The positivity of solution and the stability of the unique positive equilibrium are proved. Numerical results confirm the theoretical statements, and the sensitivity analysis shows the correlation between equilibrium populations and the parameters. Finally the effects of migration rates and death rates of hosts and ticks are explored, and migration rate has a strong positive correlation with tick and host populations.

The current model can be extended to more complicated situations. For example, the parameter \hat{q} can depend on the population of host, and seasonality can be included in the birth and death rates. Comparison with real data from Canada (such as British Columbia) and USA is ongoing, which could provide more insights into the effects of various parameters. We are also planing to include the life stages, age structure and multiple patches in the model in a future study.

Acknowledgements

This work is partially supported by NSERC (CA).

References

- [1] B.E. Anderson, K.G. Sims and J.G. Olson et al., *Amblyomma americanum: a potential vector of human ehrlichiosis*, The American journal of tropical medicine and hygiene, 1993, 49(2), 239–244.
- [2] G. Baygents and M.Bani-Yaghoub, *A mathematical model to analyze spread of hemorrhagic disease in white-tailed deer population*, Journal of Applied Mathematics and Physics, 2017, 5(11), 2262–2282.
- [3] F. Black and M. Scholes, *The pricing of options and corporate liabilities*, Journal of Political Economy, 1973, 81(3), 637–654.
- [4] S.M. Blower and H. Dowlatabadi, *Sensitivity and uncertainty analysis of complex models of disease transmission: an hiv model, as an example*, International Statistical Review/Revue Internationale de Statistique, 1994, 229–243.
- [5] T. Caraco, S. Glavanakov and G. Chen et al., *Stage-structured infection transmission and a spatial epidemic: a model for lyme disease*, The American Naturalist, 2002, 160(3), 348–359.
- [6] D. Chen, H. Wong and P. Belanger et al., *Analyzing the correlation between deer habitat and the component of the risk for lyme disease in eastern ontario, canada: A gis-based approach*, ISPRS International Journal of Geo-Information, 2015, 4(1), 105–123.
- [7] S.P. Commins and T.A. Platts-Mills, *Delayed anaphylaxis to red meat in patients with ige specific for galactose alpha-1, 3-galactose (alpha-gal)*, Current allergy and asthma reports, 2013, 13(1), 72–77.
- [8] S.P. Commins, S.M. Satinover and J. Hosen et al., *Delayed anaphylaxis, angioedema, or urticaria after consumption of red meat in patients with ige antibodies specific for galactose- α -1, 3-galactose*, Journal of Allergy and Clinical Immunology, 2009, 123(2), 426–433.
- [9] D. Earn, F. Brauer, P. van den Driessche and J. Wu, *Mathematical epidemiology*, Springer Berlin, 2008.
- [10] H.M. Feder Jr, D.M. Hoss and L. Zemel et al., *Southern tick-associated rash illness (stari) in the north: Stari following a tick bite in long island, new york*, Clinical Infectious Diseases, 2011, 53(10), e142–e146.
- [11] H. Gaff and E. Schaefer, *Metapopulation models in tick-borne disease transmission modelling*, in *Modelling Parasite Transmission and Control*, Springer, 2010, 51–65.
- [12] H.D. Gaff and L.J. Gross, *Modeling tick-borne disease: a metapopulation model*, Bulletin of Mathematical Biology, 2007, 69(1), 265–288.
- [13] J. Goddard and A.S. Varela-Stokes, *Role of the lone star tick, amblyomma americanum (l.), in human and animal diseases*, Veterinary parasitology, 2009, 160(1-2), 1–12.
- [14] B. Gomero, *Latin hypercube sampling and partial rank correlation coefficient analysis applied to an optimal control problem*, 2012.

- [15] D. Haile and G. Mount, *Computer simulation of population dynamics of the lone star tick, amblyomma americanum (acari: Ixodidae)*, Journal of medical entomology, 1987, 24(3), 356–369.
- [16] J.M. Heffernan, Y. Lou and J. Wu, *Range expansion of ixodes scapularis ticks and of borrelia burgdorferi by migratory birds*, Discrete Contin Dyn Syst Ser B, 2014, 19, 3147–3167.
- [17] A. Hoch, R. Barker and J.A. Hair, *Measurement of physical parameters to determine the suitability of modified woodlots as lone star tick habitat*, Journal of medical entomology, 1971, 8(6), 725–730.
- [18] T.R. Hofmeester, H. Sprong and P.A. Jansen et al., *Deer presence rather than abundance determines the population density of the sheep tick, ixodes ricinus, in dutch forests*, Parasites & vectors, 2017, 10(1), 433.
- [19] C.J. Holderman and P.E. Kaufman, *Lone star tick amblyomma americanum (linnaeus)(acari: Ixodidae)*, EENY580, Entomol. Nematol. Dept. UF/IFAS Extension, Gainesville, FL, 2014.
- [20] A. Kaizer, S. Foré, H.J. Kim and E. York, *Modeling the biotic and abiotic factors that describe the number of active off-host amblyomma americanum larvae*, Journal of Vector Ecology, 2015, 40(1), 1–10.
- [21] J.L. Kennedy, A.P. Stallings and T.A. Platts-Mills et al., *Galactose- α -1, 3-galactose and delayed anaphylaxis, angioedema, and urticaria in children*, Pediatrics, 2013, 131(5), e1545.
- [22] J.K. Khoury, N.C. Khoury and D. Schaefer et al., *A tick-acquired red meat allergy: A case series*, The American journal of emergency medicine, 2017.
- [23] T.M. Kollars, J.H. Oliver, L.A. Durden and P.G. Kollars, *Host associations and seasonal activity of amblyomma americanum (acari: Ixodidae) in missouri*, Journal of Parasitology, 2000, 86(5), 1156–1160.
- [24] M. LABUDA, V. DANIELOVA, L.D. JONES and P.A. NUTTALL, *Amplification of tick-borne encephalitis virus infection during co-feeding of ticks*, Medical and veterinary entomology, 1993, 7(4), 339–342.
- [25] K. Liu, Y. Lou and J. Wu, *Analysis of an age structured model for tick populations subject to seasonal effects*, Journal of Differential Equations, 2017, 263(4), 2078–2112.
- [26] S. Marino, I.B. Hogue, C.J. Ray and D.E. Kirschner, *A methodology for performing global uncertainty and sensitivity analysis in systems biology*, Journal of theoretical biology, 2008, 254(1), 178–196.
- [27] G. Mount, D. Haile, D. Barnard and E. Daniels, *New version of ltsim for computer simulation of amblyomma americanum (acari: Ixodidae) population dynamics*, Journal of Medical Entomology, 1993, 30(5), 843–857.
- [28] M.P. Nelder, C.B. Russell and K.M. Clow et al., *Occurrence and distribution of amblyomma americanum as determined by passive surveillance in ontario, canada (1999–2016)*, Ticks and tick-borne diseases, 2019, 10(1), 146–155.
- [29] N. Ogden, A. Maarouf and I. Barker et al., *Climate change and the potential for range expansion of the lyme disease vector ixodes scapularis in canada*, International journal for parasitology, 2006, 36(1), 63–70.

- [30] C.D. Patrick and J.A. Hair, *Oviposition behavior and larval longevity of the lone star tick, amblyomma americanum (acarina: Ixodidae), in different habitats*, Annals of the Entomological Society of America, 1979, 72(2), 308–312.
- [31] J.M. Pound, J.A. Miller and J.E. George et al., *Systemic treatment of white-tailed deer with ivermectin-medicated bait to control free-living populations of lone star ticks (acari: Ixodidae)*, Journal of medical entomology, 1996, 33(3), 385–394.
- [32] R.K. Raghavan, A.T. Peterson and M.E. Cobos et al., *Current and future distribution of the lone star tick, amblyomma americanum (l.)(acari: Ixodidae) in north america*, PloS one, 2019, 14(1), e0209082.
- [33] R. Rosa and A. Pugliese, *Effects of tick population dynamics and host densities on the persistence of tick-borne infections*, Mathematical biosciences, 2007, 208(1), 216–240.
- [34] H.H. Wang, W. Grant, P. Teel and S. Hamer, *Simulation of climate-tick-host-landscape interactions: Effects of shifts in the seasonality of host population fluctuations on tick densities*, Journal of Vector Ecology, 2015, 40(2), 247–255.
- [35] X. Wang and X. Zhao, *Dynamics of a time-delayed lyme disease model with seasonality*, SIAM J. Applied Dynamical Systems, 2017, 16, 853–881.
- [36] J.K. Weeks, *Modeling nymph lone star ticks in the changing landscape of the virginian peninsula: a tool for urban planning in the context of human health*, Undergraduate HOnors Theses. W&M Pbulish, 2013.
- [37] S.E. Wolver, D.R. Sun, S.P. Commins and L.B. Schwartz, *A peculiar cause of anaphylaxis: no more steak?*, Journal of general internal medicine, 2013, 28(2), 322–325.
- [38] X. Wu, V.R. Duvvuri and Y. Lou et al., *Developing a temperature-driven map of the basic reproductive number of the emerging tick vector of lyme disease ixodes scapularis in canada*, Journal of theoretical biology, 2013, 319, 50–61.
- [39] X. Wu et al., *Stage-structured population systems with temporally periodic delay*, Math. Meth. Appl. Sci, 2015, 38, 3464–3481.
- [40] X. Zhang, X. Wu and J. Wu, *Critical contact rate for vector–host–pathogen oscillation involving co-feeding and diapause*, Journal of Biological Systems, 2017, 25(04), 657–675.